Effect of strain gradient on the microstructure and mechanical properties of pearlitic steel

(article starts on next page)

Effect of strain gradient on the microstructure and mechanical properties of pearlitic steel

Johan Ahlström[1] and Xiaodan Zhang[2]

[1] Division of Engineering Materials, Department of Industrial and Materials Science, Chalmers University of Technology, 412 96 Gothenburg, Sweden
[2] Section of Manufacturing Engineering, Department of Mechanical Engineering, Technical University of Denmark, 2800 Kgs, Lyngby, Denmark

E-mail: johan.ahlstrom@chalmers.se

Abstract. Pearlitic steels, with a combination of good strength and wear properties, are commonly used for railway rails. The passage of trains creates large shear strain gradients in the surface layer of rails. Knowledge of the microstructural evolution and material properties as related to the shear strain in this layer is therefore important for prediction both of crack evolution and fatigue life. A bi-axial torsion-compression machine was used to deform fully pearlitic R260 rail steel test bars to create a similar gradient structure. Uniaxial tension and compression tests were performed on these pre-deformed test bars to evaluate the mechanical properties of the material. The local microstructural parameters, such as thickness of the ferrite and cementite lamellae, the dislocation density in the ferrite lamellae, the interlamellar spacing and eth local hardness at different places across the diameter of the bars, as well as microstructural evolution across the radius, were characterized. An attempt to set up a correlation between the local microstructural parameters, hardness and the macro mechanical properties is made and discussed in the present study.

1. Introduction

Railway rails are commonly made from pearlitic steel, which provides a sufficiently wear resistant, stiff and strong structure at a reasonably low cost. In production, low grade rails are rolled to shape and left to air cool. Production routes for more advanced head-hardened pearlitic rails and bainitic rails are also emerging. Due to rolling contact during loading, railway rails in service accumulate large plastic strains in the top layer of the rail head. The cyclic plastic deformation also generates residual compressive stresses and leads to orientation of the microstructure. The accumulated strain gradient is large, and the surface layer often contains cracks (termed "head checks"), which make investigation of the elastic-plastic properties of material extracted from the field difficult.

Some established methods are available to reach large plastic strain levels similar to those found in the surface of railway rail heads during service. These include wire drawing [1-3] and high pressure torsion [4]. Previous investigations of rail steels deformed using these methods have concluded that anisotropy exists in both the plastic behavior (yield surface) [5] and fracture behavior [6]. However, a reliable evaluation of the local strength is still missing. The current study serves to investigate the influence of plastic strain gradients on the local microstructure and mechanical properties, especially

from the small strain level. The results will provide the base for the extension of the present methodology to high strains.

2. Materials and experimental

The material studied is a R260 rail steel. The microstructure of this material is almost fully pearlitic (as shown in figure 1), with nominal chemical composition as shown in table 1.
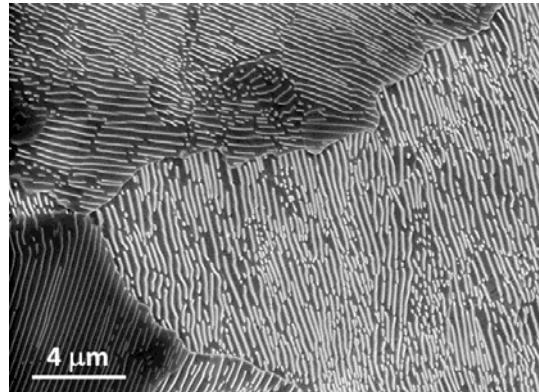

Figure 1. The pearlitic microstructure of the R260 rail steel

Table 1. Nominal chemical composition in wt-% according to ASTM E 572-13

C	Si	Mn	P	S	Cr	Al	V	N	Cu
0.72	0.31	1.04	0.006	0.010	0.02	<0.002	<0.005	0.006	0.018

2.1. Sample extraction and preparation

Test bars used to investigate the relationship between gradient structure and shear strain were extracted from rails about 20 mm below the surface of virgin rail heads. Test bars were deformed in a bi-axial machine using torsion-compression, described in detail in a previous study [7, 8]. Test bars with a gauge diameter of 10 mm were twisted 3 times ($3 \times 90°$) using 500 MPa nominal compression load (i.e. constant force, not increasing as the diameter increases). The samples for the microstructure and hardness measurement on the longitudinal cross section were taken from the middle part of the gauge section of the bars. Scanning electron microscopy (SEM), and transmission electron microscopy (TEM) have been used to characterize the microstructure. Details of the sample preparation can be found elsewhere [9-13].

2.2. Strain calculation

It is necessary to handle the strain induced by the torsional loading from different perspectives for useful characterization of deformed material properties. Using a continuum approach, it can be assumed that each plane in the original gauge section remains planar, and that the total strain imposed is proportional to the radius of each material point. In a metal though, certain slip planes become more active, and there is a distribution of strain on each cross section. In a material with strong hardening capability these differences decrease and strains are distributed more evenly, while low hardening leads to strain localization and premature fracture.

A rough measure of shear strain can be acquired using outputs from the rotational and axial displacement sensors of the test system, compensating for elastic deflections in the load train and assuming an even strain distribution in the test bar gauge section. After straining, the mantle surface of the test bar can also be studied to determine the maximum shear strain based on flow lines [8].

The focus of this study will be on three places: the center, half radius and surface of the bars. The corresponding shear strain of these three positions are 0, 0.5 and 0.7, calculated using the formula $\gamma = \tan(90 - \theta) \cdot r/R$ where θ is the measured angle at the outer surface of tested bars, r is the radius measured from the center line of the bars, and R is the final radius of the tested bars.

2.3. Microstructural characterization

Detailed microstructure characterization was carried out TEM (JEOL 2000FX) due to the fineness of the lamellar structure and sectioning problems related to the 3D lamellar pearlitic structure. Special care was taken to make sure the edge-on situation was used for determination of the parameters, such as the interlamellar spacing (ILS), the thickness of ferrite lamellae (F) and cementite lamellae (C) where ILS is the sum of F and C. Dislocation configurations were revealed by tilting the TEM foil and the densities were determined by the intersection method [1-3].

2.4. Micro-hardness measurements and mechanical testing

A Struers DuraScan 70 microhardness machine was used to conduct measurements on the test with shear strains of 0, 0.5 and 0.7 on the longitudinal cross section of the bars with a load of 500 g (HV0.5). An average value was calculated from ten indents. Tension and compress testing under strain-controlled mode was also carried out.

3. Results and discussion

3.1. Microstructure and hardness evolution

Figure 2 shows the microstructure evolution with increasing shear strain. It is clear that the number of shear bands increases with shear strain, evidenced by twisted lamellae in the microstructure. The detailed quantitative characterization of the microstructural parameters is shown in table 2. The key microstructural parameters such as ILS, F and C decrease by only several percent. However, the hardness shows a large increase with shear strain (see table 3), which indicates the change of another microstructural parameter, namely the dislocation density.
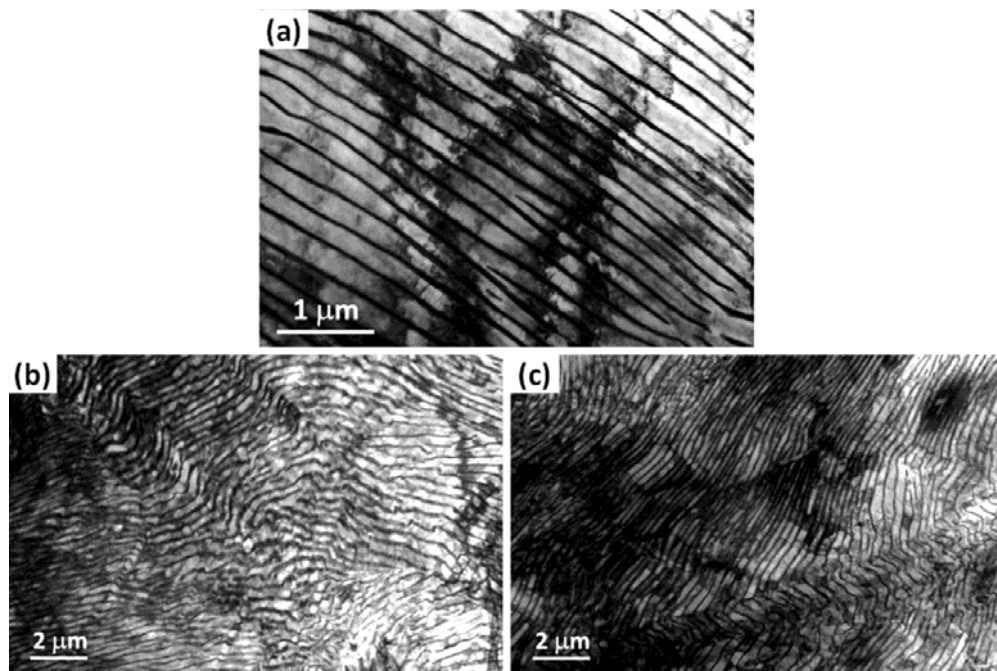

Figure 2. TEM micrographs at positions corresponding to strains of 0 (a), 0.48 (b) and 0.67 (c) of the 3-turns bar, show the alternating ferrite and cementite lamellae. The horizontal direction corresponds to the bar axis.

Table 2. ILS and thickness of ferrite (F) and cementite (C) versus shear strain [8]

Shear strain	ILS (nm)	F (nm)	C (nm)

0	233 ± 39	193 ± 30	40 ± 6.5
0.5	223 ± 40	184.1 ± 39	38.9 ± 8
0.7	224 ± 33	188.4 ± 35	35.6 ± 7.1

Table 3. Microhardness (HV0.5) versus shear strain [8]

Shear strain	Microhardness (HV0.5)
0	288 ± 9.8
0.5	337 ± 15.8
0.7	345 ± 14.8

3.2. Dislocation density

At the small strains investigated in the present study, shear-introduced twisting of the lamellar structure is observed (see figures 2b and 2c). This twisting-related reorientation of the lamellar structure to be vertical to the bar axis is just starting, and is not as severe as seen in pearlitic steel wires drawn to large strains [14, 15] which involves shear banding and curling [16, 17]. Such obvious heterogeneity in the heavily-drawn wires has not been observed in the present case at small strains. As such, the following analysis will be based on the assumption of a lamellar structure and the values of microstructural parameters including dislocation densities will be average values, which also allow the comparison of the present data with the reported data of deformed pearlite in the literature.

In a lamellar structure with alternating soft ferrite and hard cementite lamellae, the plastic deformation is largely controlled by the ferrite lamellae, where the slip initially starts in the ferrite and is then transferred into the cementite [18]. Table 4 shows the increase of dislocation density in the ferrite lamellae with increasing shear strain, while examples of the detailed dislocation configurations are shown in figure 3. The dislocations are of threading and tangled configuration, with bulging from the ferrite/cementite interfaces also seen. Threading dislocations were also observed in the original sample at a relative high dislocation density of 6.0×10^{13} m^{-2}. This high dislocation density may have its cause in the difference of the thermal expansion coefficient of the two phases in, in the semi-coherent interfaces and in elastic compatibility between the two phases [18-20].

Table 4. Dislocation density in the ferrite lamellae versus the shear strain [8]

Shear strain	Average dislocation density (m^{-2})
0	6.0×10^{13}
0.5	2.4×10^{14}
0.7	3.1×10^{14}

40th Risø International Symposium on Material Science

IOP Conf. Series: Materials Science and Engineering **580** (2019) 012027

IOP Publishing
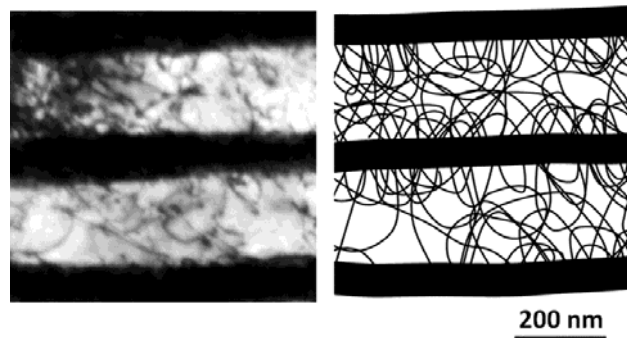
doi:10.1088/1757-899X/580/1/012027

Figure 3. TEM micrograph and sketch showing dislocation configurations in the ferrite lamellae, where the thick black lines represent cementite lamellae and the thin black lines represent dislocations in the ferrite lamellae [8].

3.3. Structure-strength relationship

The quantified microstructural parameters including ILS, F and C (table 2) shows the changes are small for small shear strains in the present case. Accordingly, the hardness increase with shear strain has its major cause in the increase of dislocation density in the ferrite lamellae. The increment of the local strength can be evaluated through the calculated flow stresses from microstructural parameters deduced from the primary flow stress. The microstructural characterization suggests the following two strengthening mechanisms: boundary strengthening related to the ferrite thickness, F, where the cementite lamellae are taken as barriers for dislocation pile-ups, described by $\sigma(b) = k \cdot (2F)^{-0.5}$, where k is the Hall-Petch constant; and dislocation strengthening related to the dislocation density, described by $\sigma(\rho) = M\alpha Gb\sqrt{\rho}$, where M is the orientation factor, taken as $3, \alpha = 0.24, G = 78\ GPa$ is the shear modulus, and b is the burgers vector, taken as 0.248 nm.

On the assumption that these strength contributions can be additive, the flow stress can be expressed as:

$$\sigma = \sigma_0 + \sigma(b) + \sigma(\rho) \tag{1}$$

where σ_0 is the friction stress, taken as 60 MPa [2, 3].

The above calculation of the local strength increment with the shear strain will be compared with the experimental evaluation from the hardness increment via the following formula:

$$\Delta\sigma_{HV} = \Delta HV_{0.5}/k_{HV} \tag{2}$$

where $k_{HV} = 3.3 \pm 0.4$, consistent with hypo eutectoid steels [21], deformed pearlitic steel at low and medium strains [22], and deformed metals with lamellar dislocation structures at medium and large strains [23-26]. The comparison is shown in table 5. Taking into account the standard deviation, a good agreement is found between the measured strength increment by hardness and the calculated strength increase from quantified microstructural parameters.

Table 5. Local strength increase versus the shear strain [8]

Shear strain	$\Delta\sigma_{cal}$ (MPa)	$\Delta\sigma_{HV}$ (MPa)
0.5	117	146 ± 29
0.7	141	169 ± 44

4. Conclusion

To develop a microstructure-based methodology for evaluation of the local strength and mechanical response of rail surface layers after run-in, a bi-axial torsion-compression machine has been used to deform test bars of R260 pearlitic rail steel to low shear strains. The evolution of local microstructure and local strength with shear strain has been systematically characterized and quantified by TEM and microhardness. The following conclusions can be made:

- The interlamellar spacing, and the thickness of the ferrite and cementite lamellae, only show a small decrease up to a shear strain of 0.7.
- The observed hardness increase with the shear strain is due to the increase of dislocation density in the ferrite lamellae, where the main dislocation configurations are threading dislocations and dislocation tangles.
- Two strengthening mechanisms, namely boundary strengthening and dislocation strengthening, are proposed to account for the results, based on microstructural characterization. Based on the linear additivity of the contributions from these two strengthening mechanisms, good agreement is found between the measured strength increment seen in hardness measurements and the calculated strength increase determined using the quantified microstructural parameters.

Acknowledgements

References

[1]   Zhang X, Hansen N, Godfrey A and Huang X 2018 *Mater Sci Technol* **34** 794
[2]   Zhang X, Hansen N, Godfrey A and X Huang 2016 *Acta Mater.* **114** 176
[3]   Zhang X, Godfrey A, Huang X, Hansen N and Liu Q 2011 *Acta Mater* **59** 3422
[4]   Pippan R, Wetscher F, Hafok M, Vorhauer A and Sabirov I 2006 *Adv Eng Mater* **8** 1046
[5]   Cvetkovski K and Ahlström J 2013 *Wear* **300** 200
[6]   Kapp M, Hohenwarter A, Wurster S, Wang B and Pippan R 2016 Acta Mater 106 239
[7]   Meyer K A, Nikas D and Ahlström J 2018 *Wear* **396–397** 12
[8]   Nikas D, Zhang X and Ahlström J 2018 *Mater Sci Eng A* **737** 341
[9]   Chen S, Hu J, Zhang X, Dong H and Cao W 2015 *J Iron Steel Res Int* **22** 1126
[10] Fan G H, Wang Q W, Du Y, Geng L, Hu W, Zhang X and Huang Y D 2014 *Mater Sci Eng A* **590** 318
[11] Zhang X D, Liu W, Godfrey A and Liu Q 2009 *Metall. Mater. Trans. A* **40** 2171
[12] Zhang X, Godfrey A, Huang X, Hansen N, Liu W and Liu Q 2009 *30th Risø international symposium on materials science: nanostructured metals – fundamentals to applications* (Risø, Denmark) p 409
[13] Zhang X, Godfrey A, Hansen N, Huang X, Liu W and Liu Q 2010 *Mater Charac* **61** 65
[14] Zhang X, Hansen N, Godfrey A and Huang X 2012 *33rd Risø international symposium on materials science: Nanometals – status and perspectives* (Risø, Denmark) p 407
[15] Zhang X, Hansen N, Godfrey A and Huang X 2014 *35th Risø International Symposium on Materials Science: New Frontiers of Nanometals* (Risø, Denmark) p 153
[16] Langford G 1977 *Metall Trans A* **8** 861
[17] Zhang X, Godfrey A, Hansen N, Huang X, Liu W and Liu Q 2010 *Mater. Charac* **61** 65
[18] Zhang X D, Godfrey A, Liu W and Liu Q 2011 *Mater. Sci. Techno* **27** 562
[19] Dollar M, Bernstein I M and Thompson A W 1988 *Acta Metall* **36** 311
[20] Zhang X, Godfrey A, Hansen N and Huang X 2013 *Acta Mater* **61**, 4898
[21] Pavlina E J and Van Tyne C J 2008 *J Mater Eng Perform* **17** 888
[22] Zhang X 2009 Quantitative Investigation of Microstructural Evolution During the Cold Wire-drawing of a Pearlitic Steel Wire and its Relationship with Mechanical Properties, Tsinghua University, Beijing
[23] Meyers M A and Chawla K K 2009 *Mechanical Behavior of Materials*, Cambridge University Press, Cambridge, p 223
[24] Zhang X, Hansen N, Gao Y and Huang X 2012 *Acta Mater* **60** 5933
[25] Zhang X, Hansen N and Nielsen C V 2017 *Local microstructure and flow stress in deformed metals* in: IOP Conference Ser: Mater Sci Eng, **219** 012053
[26] Zhang X, Nielsen C V, Hansen N, Silva C M A and Martins P A F 2019 *Int. J. Plast.* **115** 93